First-principles study of benzene adsorption on the SiC(001)-(3×2) surface

Jürgen Wieferink,* Peter Krüger, and Johannes Pollmann
Institut für Festkörpertheorie, Universität Münster, 48149 Münster, Germany
(Received 1 July 2008; revised manuscript received 21 August 2008; published 17 October 2008)

Adsorption of benzene on the SiC(001)-(3×2) surface is investigated employing density-functional theory within the generalized gradient approximation. Due to the relatively large Si dimer distance on the clean surface, benzene appears to adsorb only in a standard-butterfly configuration on single dimers. Such a well-defined structure might turn out to be of particular interest for fundamental experimental investigations as well as for surface functionalization by organic molecules. The reaction pathway of benzene from an initial state in vacuum to the final adsorption state in the standard-butterfly configuration on the surface is explored and the reaction process is analyzed employing maximally localized Wannier functions. The electronic structure of the optimized adsorption configuration is discussed in terms of the surface-band structure, charge and state densities, as well as scanning tunneling microscopy images.

DOI: 10.1103/PhysRevB.78.165315 PACS number(s): 68.43.Fg, 68.43.Bc, 73.20.Hb

I. INTRODUCTION

Within the last decade there is an ever increasing technological interest in organic functionalization of semiconductor surfaces.[1,2] Three requirements have to be met to allow for surface functionalization using specific combinations of organic molecules and semiconductor surfaces. Obviously, in the first place, the employed organic molecules have to adsorb on the semiconductor surface at all. Second, an intact functional group has to remain upon adsorption which is exposed outside. Last, but not the least, the surface should remain to be well defined after adsorption, which is most easily achieved by adsorbing a self-ordering organic monolayer.

As a prototype for the interaction of an aromatic hydrocarbon with a semiconductor surface, adsorption of benzene on Si(001)-(2×1) has been a subject of a considerable number of experimental and theoretical studies.[3–22] Due to the fact that the distance between neighboring dimers on the Si(001)-(2×1) surface is of about the same size as the spatial extent of a benzene molecule (C_6H_6), the latter may adsorb on a single dimer or it may bridge two adjacent dimers. Correspondingly, several adsorption structures exist (for a review, see Ref. 10; and for some more recent geometry suggestions, see Ref. 11). Most experimental studies agree that benzene initially adsorbs in a single-dimer geometry with two C—Si σ bonds between opposing carbon atoms of the molecule and the Si atoms of a dimer leading to a 1,4-cyclohexadienelike standard-butterfly (SB) structure. For lower coverages or nonvicinal surfaces, a subsequent conversion to a bidimer structure is seen on the time scale of minutes.[4,7,9,21] The nature of the bidimer structure is still under debate. Density-functional supercell calculations[10,11,13,17,20,22] yield very similar adsorption energies for the most favorable adsorption sites. The recent generalized gradient calculation of Johnston *et al.*[22] shows that inclusion of van der Waals interaction has a crucial influence on the order of these adsorption energies. Despite all experimental and theoretical efforts, the definite adsorption structure of benzene on Si(001)-(2×1) appears still to be a matter of discussion.

The situation is more clear-cut for the SiC(001)-(3×2) substrate surface. It also features asymmetric Si dimers on the top layer whose local bonding configuration is very similar to that on Si(001). However, the distance of 6.2 Å between neighboring dimers at SiC(001)-(3×2) is much larger than that (3.9 Å) on Si(001)-(2×1). This simple geometrical fact has a vital influence on benzene adsorption at SiC(001)-(3×2) in that it rules out most of the adsorption models discussed for benzene on Si(001). According to our results, C_6H_6 adsorbs on SiC(001)-(3×2) only in one well-defined equilibrium structure: the standard-butterfly configuration, as we will show in this work. In this configuration, the adsorbed benzene molecules retain two unsaturated π bonds which can become operative in chemical functionalization of the system. Therefore, benzene on SiC(001)-(3×2) might become a useful role model for studies of organic functionalization of semiconductor surfaces. By the same token, the structural uniqueness of the system suggests that a well-ordered benzene monolayer should readily be achievable on this surface in experiment.

While there have been studies of acetylene,[23] ethylene,[24] and 1,3-cyclohexadiene[25] on SiC(001)-(3×2), to the best of our knowledge benzene adsorption on this surface has not been studied before. We have, therefore, investigated the reaction of benzene with the SiC(001)-(3×2) surface in detail.

This paper is organized as follows. In Sec. II we briefly address the methods used in our calculations, i.e., density-functional theory (DFT) within the generalized gradient approximation (GGA), the modeling of the adsorbate system, the quadratic string method (QSM) for calculating reaction pathways and finding reaction barriers, and the calculation of maximally localized Wannier functions (MLWFs) for the discussion of the charge density. In Sec. III we present and discuss our results. We identify the most favorable adsorption site for benzene on SiC(001)-(3×2) and explore the minimum-energy pathway (MEP) to the final adsorption state. The reaction process of benzene with the surface is further examined with the help of maximally localized Wannier functions. Finally, the electronic structure of the C_6H_6:SiC(001)-(3×2) adsorption system is discussed. A short summary concludes the paper.

II. METHODS

The calculations are performed within density-functional theory[26,27] using the GGA with the exchange-correlation functional, as suggested by Perdew and Wang[28] (PW 91). Norm-conserving separable pseudopotentials[29] are employed and the wave functions are expanded in Gaussian orbitals of s, p, d, and s^* type with decay constants given in Ref. 23. The charge density, as well as the local parts of the potential, is represented by Fourier series. For an efficient evaluation of these terms the algorithms presented in Ref. 24 are used.

The C_6H_6:SiC(001)-(3×2) adsorbate system is modeled within the supercell approach. Each supercell contains a slab consisting of one benzene adlayer, ten SiC substrate layers, and a layer of hydrogen atoms saturating the bottom layer of the slab. The slabs are separated by at least 8 Å of vacuum between the uppermost adsorbate atom in one supercell and the saturating hydrogen layer in the next supercell in each case. All atoms in the benzene monolayer and on the first five substrate layers are fully relaxed during structure optimization and reaction pathway calculations. Brillouin-zone integrations are carried out using 16 special **k** points.

The basis set superposition error in the interaction and adsorption energies is reduced, employing a larger basis set for the adsorbate and surface atoms, as discussed in Ref. 23. The remaining error is corrected using the counterpoise scheme described by Boys and Bernardi.[30] These corrections also account for the superposition error that originates from the interaction of the periodic images of the adsorbate with each other. This is achieved using a larger supercell during the correction calculations.

For finding reaction pathways we have implemented the QSM of Burger and Yang.[31] The key idea of this method and its predecessor, the string method of E *et al.*,[32] is somewhat similar to the nudged elastic band (NEB) method of Henkelman and Jónsson.[33–35] In contrast to the NEB method, the string method uses a numerical integration scheme along the forces perpendicular to the tangents to direct the images to the minimum-energy path. In order to avoid numerical problems, no spring force is used but the images are respaced on a spline interpolation when needed. The QSM in turn performs the integration along the force of a local approximative quadratic expansion of the potential-energy surface. Thus the DFT functional is only evaluated from time to time to update the expansion function. The QSM has the additional advantage that one may use chemically motivated models[36] for the initial guess of the second-order terms of the expansion. We have convinced ourselves[37] that the QSM is competitive with the algorithms compared by Sheppard *et al.*[38] However, the QSM cannot be generalized to a climbing image method without a huge loss of performance.

In order to discuss formal charges, charge transfer, and chemical bonding in final adsorption states and along a reaction pathway, we determine maximally localized Wannier functions.[39] These provide an insightful chemical picture of the bonding properties. The construction of the Wannier functions is achieved by interfacing our code to the WANNIER90 package of Mostofi *et al.*[40] The Wannier functions calculated by this program partition the charge density into contributions of chemically meaningful orbitals. Especially the centers of the Wannier functions are very useful to shed light on the charge redistribution in an adsorbate system along a reaction pathway. A Wannier center is the expectation value of the position operator with respect to a Wannier function. For covalent systems, it acts like a link between atoms, indicating the presence of a chemical bond.

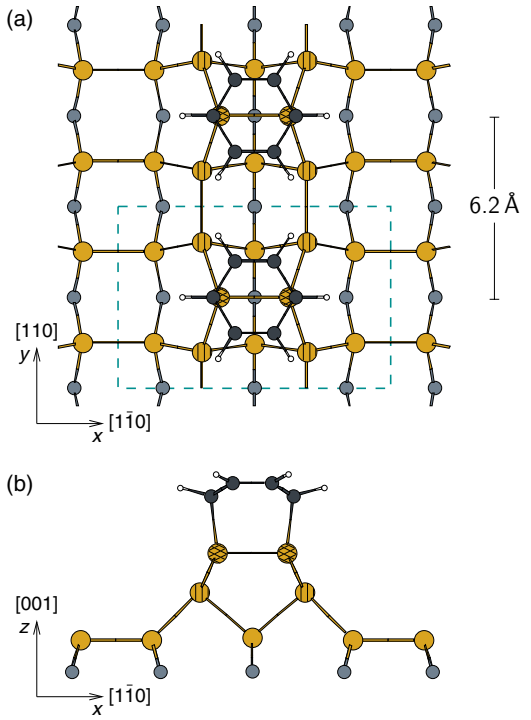

FIG. 1. (Color online) Top (a) and side (b) views of optimized standard-butterfly structure of benzene on SiC(001)-(3×2). Large ocher (light gray) circles denote Si atoms while substrate carbon atoms are shown as small bright blue (gray) circles. The density of the shadings of Si atoms increases with ascending height. Small blue (dark gray) circles and white dots depict C and H atoms in the benzene molecule, respectively. The dashed cyan (gray) line shows a 3×2 surface unit cell.

In an accompanying study, we have investigated benzene adsorption on the Si(001)-(2×1) surface. Our results compare very well with those of previous DFT-GGA calculations. Therefore, we are confident that the theoretical methods employed in this work are also applicable to describe benzene adsorption on the SiC(001)-(3×2) surface.

III. RESULTS AND DISCUSSION

A. Adsorption geometry

The clean substrate surface is described by the two-adlayer asymmetric dimer model,[41] which is widely accepted[42,43] by now. The model features a Si-terminated SiC(001)-(3×2) surface covered with two partial Si adlayers with one-third and two-third monolayer coverage from top to bottom as can be seen in Fig. 1. The two top-layer Si atoms per 3×2 unit cell form one asymmetric dimer in the $3\times$ direction which exposes both an electron pair donor and an electron pair acceptor, namely, the dangling bonds at the dimer up and down atoms, respectively. On the second

adlayer, four Si atoms form two weak Si dimers in the ×2 direction. The Si atoms on the third layer, which is the first complete layer of the substrate, form weak dimers in the 3× direction again. The dimers on the second and third layers are fully saturated. Therefore, the model has only two unsaturated surface dimer dangling bonds per unit cell that constitute the reactive units of the structure.

As noted already in Sec. I, benzene can only adsorb on a single dimer at the SiC(001)-(3×2) surface because the dimer distance of 6.2 Å is too large to allow for bidimer configurations. Therefore, only two of the benzene adsorption models discussed for Si(001) in the literature[3–22] remain as candidates for nondissociative adsorption of benzene on SiC(001)-(3×2). In the first model, two *neighboring* C atoms of the molecule bind to a single dimer and the molecule is tilted with respect to the surface normal. For this tilted model, constituting a 1,3-cyclohexadienelike di-σ geometry, we find a small adsorption energy of 0.09 eV. The other is the SB model, which is already mentioned in Sec. I. In the SB model, benzene features a 1,4-cyclohexadienelike structure with two opposing C═C double bonds. The remaining two *opposing* C atoms, which do not participate in a double bond, are each bound to one of the Si dimer atoms, so that the bonding configuration is also a di-σ structure. The optimized bond lengths of 1.50 and 1.34 Å for the carbon single and double bonds, respectively, match the usual values for these types of bonds in hydrocarbon molecules. The adsorption energy of the SB model results as 0.83 eV.

We have performed supplementary calculations for two additional adsorption structures. First, we have considered an interlayer adsorption species such as the one discussed in Ref. 25 for 1,3-cyclohexadiene. However, we did not even find a metastable geometry of this kind for benzene on SiC(001)-(3×2). Second, we have investigated *dissociative* adsorption of benzene keeping the aromaticity of C_6H_6 intact. For instance, adsorption with a final configuration containing a phenyl group (C_6H_5) at one Si dimer atom and a H atom at the other involves an adsorption energy of 1.47 eV, which is larger than that of the *nondissociative* adsorption in SB configuration indeed. The respective dissociation process, however, turns out to be very unlikely due to an energy barrier of about 0.8 eV.

The relative size of the adsorption energies of the tilted and the standard-butterfly models (0.09 and 0.83 eV, respectively) clearly reveals that the tilted model is very unfavorable. Thus, there seems to be only one realistic adsorption structure for benzene on SiC(001)-(3×2): the SB geometry. The respective optimized structure is shown by a top and a side view in Fig. 1. Clearly, the top-layer Si dimers of the substrate surface become symmetric upon benzene adsorption in the SB configuration. The length of the C—Si bonds between the molecule and the substrate is 1.97 Å and the bond length of the Si dimer is 2.35 Å. The SB structure is characterized by an adsorption energy of 0.83 eV for saturation coverage of one molecule per (3×2) cell, as noted above, and by 0.93 eV for half of this coverage calculated in a $c(6\times4)$ cell, respectively. The energy difference of 0.1 eV is a result of the nearest-neighbor Pauli repulsion between H atoms which reside for monolayer coverage at the rather small distance of 2.00 Å in adjacent 3×2 cells (see top view in Fig. 1). For the respective coverages of benzene in SB configuration on Si(001)-(2×1), the adsorption energies resulting from our accompanying calculations are of the same order (0.88 and 0.90 eV, respectively) because the local topology of the Si dimers and the bonding topology of the benzene molecules are very similar. In the latter case the benzene molecules in SB sites are adsorbed on second-nearest-neighbor dimers at saturation coverage, so that the respective distance between the interacting H atoms is as large as 3.5 Å. As a result, the difference between the adsorption energies of the two coverages is correspondingly smaller.

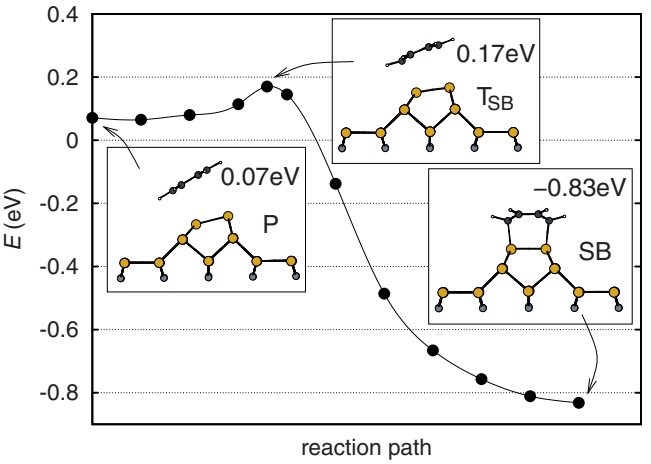

FIG. 2. (Color online) Minimum-energy path from the precursor (see Ref. 44) through the transition to the final standard-butterfly state. The insets show side views of the respective atomic configurations. The interaction energies are counterpoise corrected. For further details, see caption of Fig. 1.

B. Reaction process

So far we have seen that the SB configuration is by far the most favorable final adsorption structure. But this does not yet mean that there is actually a viable reaction pathway for the benzene molecules on which they can reach this final terminal position in a real experiment. To resolve this question we have calculated the MEP, shown in Fig. 2, from a precursor state[44] to the final SB adsorption state. The insets show side views of the atomic configuration in the precursor (P), the transition (T_{SB}), and the final SB states. It turns out that there is a small energy barrier between the precursor and the transition state of 0.10 eV. When the molecule comes closer to the surface, a very significant energy gain occurs due to formation of two C—Si σ bonds between the molecule and the substrate. The molecule eventually attains the SB structure. The small energy barrier related to the transition state may be considered as an indication that benzene physisorbs at very low temperatures and only chemisorbs at a higher temperature. This conjecture is based on related behavior of benzene on Si(001)-(2×1) where the molecule has been observed to initially physisorb at 100 K and chemisorb upon annealing to 200 K.[9,21] In the case of Si(001)-(2×1) we find a very similar barrier of 0.11 eV for the respective transition state. Thus, it appears that benzene adsorption

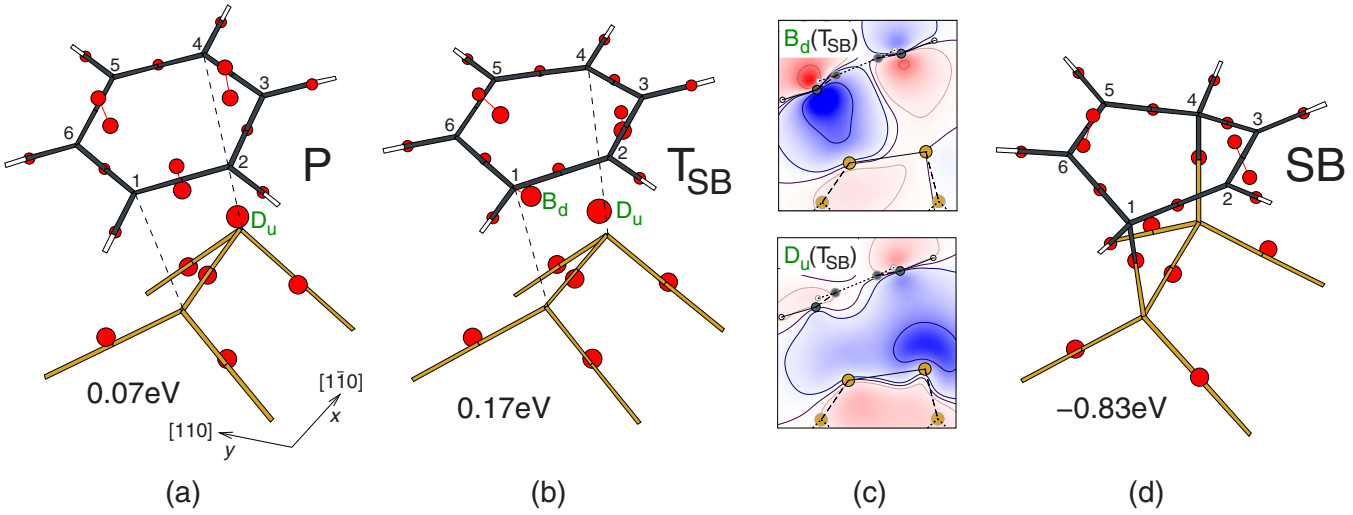

FIG. 3. (Color online) Wannier centers for precursor, transition, and final SB geometries of the C_6H_6:SiC(001)-(3×2) adsorption system. Only the benzene molecule, the topmost dimer, and its back bonds are shown. Each Wannier function is represented by a red dot positioned at its center. The size of the dots is proportional to the spread of the Wannier function. For clarity no circles are drawn for atoms. They reside at the junctions of the bonds, whose color code is the same as in Figs. 1 and 2. Below the structure figures, the respective counterpoise-corrected interaction energies are given. Additionally, in panel (c), the two most prominent Wannier functions of the transition geometry are plotted in the plane containing the silicon dimer. Contour lines are plotted at 0, $\pm 0.01 a_B^{-3/2}$, and $\pm 0.1 a_B^{-3/2}$. Bonds lying within, outside, and with an angle to the plotting plane are shown in panel (c) by solid, dotted, and dashed lines, respectively.

on SiC(001)-(3×2) in the well-ordered SB configuration should readily be realizable in experiment at room temperature.

As a side remark, we mention that our calculations can also be considered as a test case for the QSM. For the path from P to SB, 23 DFT force calculations per image were needed until all force components perpendicular to the tangents are converged to 6×10^{-4} Ry/a_B. A typical NEB calculation using the proposed quenched molecular-dynamics scheme[33] would need several hundred force calculations for the same degree of accuracy. The QSM exhibits a rapid convergence but is not particularly robust for larger systems.[46]

Using maximally localized Wannier functions, we now address the transition from the precursor to the final SB structure in more detail. Figure 3(a) shows the precursor state P. The distances between the C atoms C_1 and C_4 and the dimer down and up atoms are 2.89 and 3.58 Å, respectively. So there is no covalent bond between the molecule and the surface established yet. The substrate is essentially undistorted and the molecule is flat but slightly rotated toward the dimer down atom. Figure 3 additionally shows the positions of the centers of the MLWFs. The charge density of the benzene precursor is distributed among six C—H bonds and nine orbitals in the aromatic ring. The latter split into alternating single and double bonds. This partitioning is degenerate with the one rotated by 60°. It is interesting to note that, when analyzing the electronic structure with MLWFs, a double bond is not split into a σ and a π bond but into two so-called banana-shaped bonds because the corresponding Wannier functions are more localized.

All Si—Si bonds including the dimer bond consist of one orbital each and there is an additional orbital belonging to the occupied dangling bond at the dimer up atom. Since the Wannier functions are used to span the linear space of the *occupied* orbitals, there is no Wannier center at the dangling bond of the dimer down atom.

As the molecule approaches the dimer, the aromaticity of the benzene ring becomes distorted leading to an increase in the energy by 0.10 eV. In the transition state T_{SB}, shown in Fig. 3(b), the C—Si distances to the dimer down and up atoms reduce to 2.44 and 3.08 Å, respectively. There are two Wannier functions related to these emerging bonds, which are plotted in panel (c) of Fig. 3 and labeled B_d and D_u, respectively. The B_d Wannier function (near C_1) is induced by the interaction of the molecule with the empty dangling bond at the dimer down atom, which pulls charge out of the benzene ring. In the idealized view of a σ complex, an intermediate in an electrophilic reaction, the B_d orbital is completely used to establish a C—Si bond to the dimer down atom. In the ring, six σ as well as two π orbitals and a positive formal charge remain. The latter is stabilized by the conjugacy of the π bonds and mainly localized at the ortho-positions (C_2 and C_6) and paraposition (C_4), which manifests itself in the position of the Wannier centers of the π orbitals at the meta-atoms (C_3 and C_5) shown in Fig. 3(b). The charge loss in the ring leads to an interaction of the occupied dangling-bond orbital at the dimer up atom D_u with the para-atom C_4, as can be seen in the lower panel of Fig. 3(c).

In the final adsorption geometry (SB), shown in Fig. 3(d), the states B_d and D_u have evolved to C—Si σ bonds. Their bond length is 1.97 Å. The two remaining π bonds of the ring together with the respective σ bonds set up the C_2=C_3 and C_5=C_6 double bonds.

C. Electronic structure

We now turn to the electronic structure of C_6H_6:SiC(001)-(3×2) in the SB geometry. The band struc-

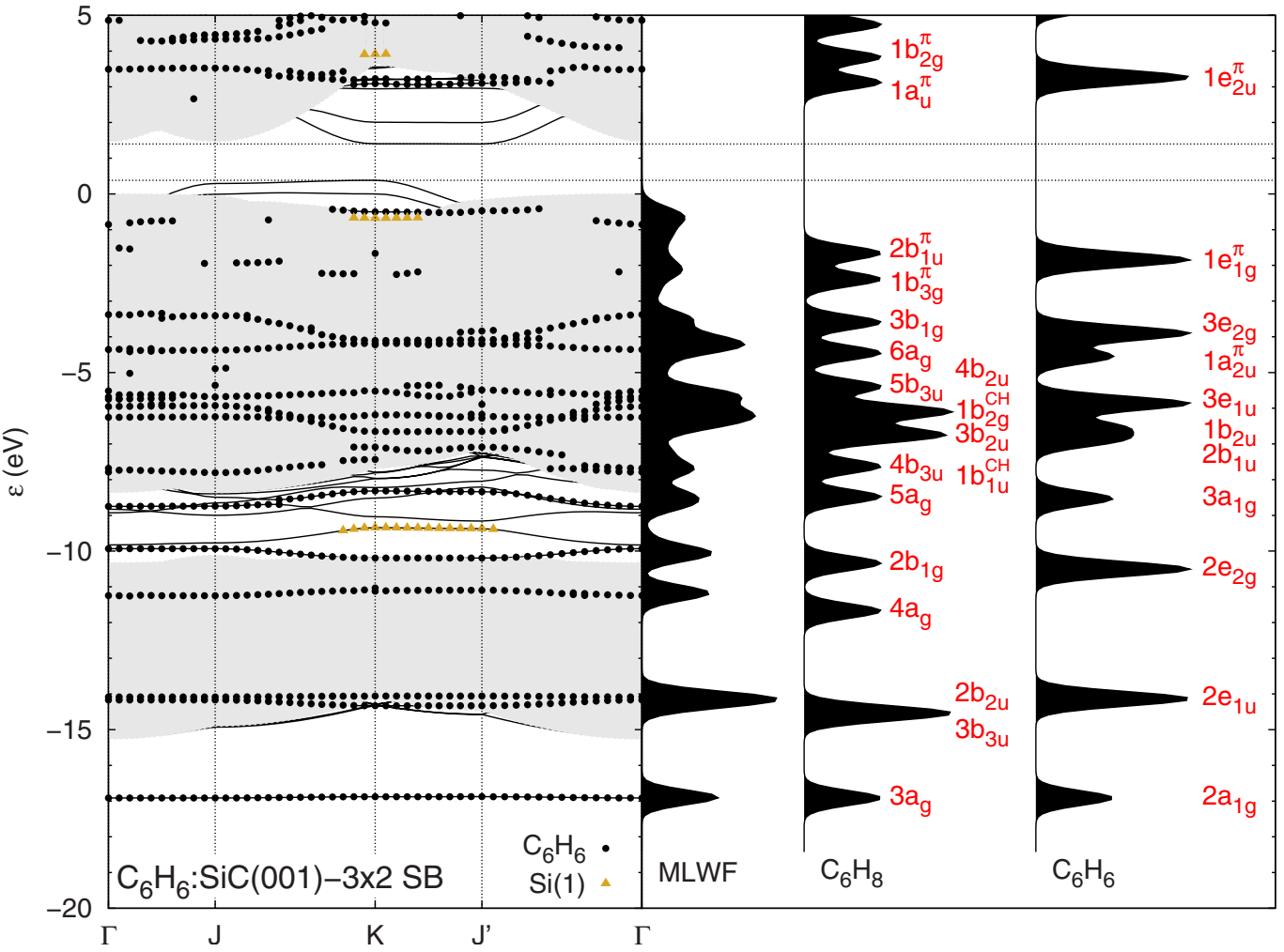

FIG. 4. (Color online) Electronic structure of the C_6H_6:SiC(001)-(3×2) SB adsorption system. The left section shows the band structure with benzene-derived bands marked by black dots. Bands whose states are localized at the top Si dimer are indicated by filled ocher (gray) triangles. The projected bulk-band structure is shaded in gray. The high-symmetry points J and J' lie on the $[1\bar{1}0]$ (x) and $[110]$ (y) directions of the surface Brillouin zone, respectively. To the right, the density of states (DOS) weighted by the population of the MLWFs at the molecule and at the C—Si back bonds is shown in comparison with the DOSs of an isolated 1,4-cyclohexadiene (C_6H_8) and an isolated benzene (C_6H_6) molecule, which are shifted in energy to match the energetic position of the lowest state of the adsorbate system. The molecular states are labeled according to the irreducible representations of the D_{2h} and D_{6h} symmetry groups of the free molecules, respectively (Refs. 8 and 45). All states with a nodal plane parallel to the surface are marked by upper indices π or CH, respectively, depending on their chemical nature.

ture of the system is shown in Fig. 4 together with the local DOS, as calculated by weighting the DOS with the population of the MLWFs at the molecule and at the C—Si back bonds. To ease the discussion, we compare in Fig. 4 the band structure of the adsorbate system with the DOS of an isolated benzene molecule (C_6H_6), as well as with the DOS of an isolated 1,4-cyclohexadiene (C_6H_8) molecule, which is isoelectronic to a benzene molecule on SiC(001)-(3×2) in SB configuration. Most states of cyclohexadiene are closely related to the adsorbate-induced states of the C_6H_6:SiC(001)-(3×2) adsorption system. The peaks of the molecular DOSs are labeled by the appropriate irreducible representations of the D_{6h} (C_6H_6) and D_{2h} (C_6H_8) symmetry groups.

An isolated benzene molecule contains twelve σ and three π bonds. The σ bonds are only slightly influenced by adsorption of C_6H_6 in SB configuration. As a consequence, 12 pronounced bands occur lying between −17 and −3 eV in the band structure. The molecular π bonds, on the contrary, are significantly affected due to the interaction of C_6H_6 with the substrate.

Let us first address the different band groups among the σ bands in some more detail. Beneath −7 eV there are seven adsorbate-induced bands. The states giving rise to these bands are similar in nature to the respective states of C_6H_8. The assignment of these states to those of C_6H_6 is self-evident taking the twofold degeneracy of $2e_{1u}$ and $2e_{2g}$ into account. The MLWF weighted DOS closely resembles that of the isolated C_6H_8 molecule. In addition to the adsorbate-induced bands there exist further states within the heteropolar gap which are localized at the dimers of the two Si adlayers and the first complete Si layer of the substrate. In the

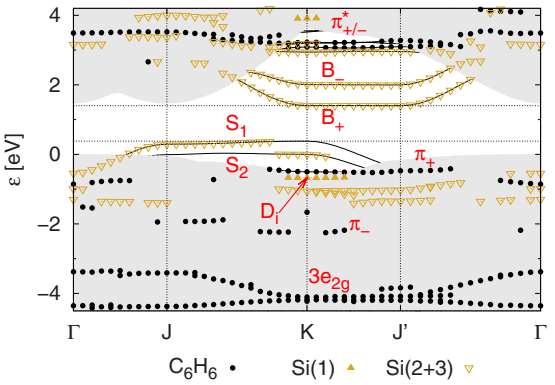

FIG. 5. (Color online) Section of the band structure near the gap energy region of C_6H_6:SiC(001)-(3×2) in SB geometry. Empty ocher (gray) triangles show states localized in the second or third Si layer. For further details, see the caption of Fig. 4.

energy range between −7 and −5 eV there are three further benzene-induced bands. Due to the large spatial extent of the $4b_{2u}$ state of C_6H_8 in y direction, the corresponding band is the most dispersive of the three bands with an energy of −6.0 eV at Γ and −6.7 eV at K. The other two bands, $3b_{2u}$ and $5b_{3u}$, both only have a width of the order of 0.1 eV. The two bands at −4.2 eV and between −4.1 and −3.4 eV correspond to the two cyclohexadiene states $6a_g$ and $3b_{1g}$, respectively. The large spatial extent of the $3b_{1g}$ state in the y direction leads to a large dispersion of 0.7 eV of the latter band as well.

As a side note, we mention that we find the same 12 adsorbate-induced σ bands for benzene adsorption in SB configuration on Si(001)-(2×1), but all of them disperse by less than 0.2 eV. This can be attributed to the respectively larger intermolecular distance of 3.50 Å in the y direction between H atoms of neighboring C_6H_6 molecules in the SB structure on Si(001)-(2×1) as compared to 2.00 Å at SiC(001)-(3×2). For a detailed discussion of the correlation between respective molecular states and surface bands at Si(001)-(2×1), see Ref. 8.

The stronger interaction between the benzene π orbitals and the Si dangling bonds of the SiC(001)-(3×2) surface gives rise to states of the adsorbate system that are related to the $1b_{1u}^{\mathrm{CH}}$ and $1b_{2g}^{\mathrm{CH}}$ back-bond states of C_6H_8. They do not appear as strong resonances in the band structure but are spread over the whole energy region from −10 to 0 eV.

The remaining two π bonds of the adsorbed benzene molecule give rise to two bands labeled as π_- and π_+ in Fig. 5, which shows an enlarged section of the band structure close to the fundamental band gap. These bands reside in the energy region between −3 and 0 eV. Due to the strong coupling of the molecular orbitals to the substrate states, these bands are discernible in parts of the Brillouin zone only. This is not surprising since both the π bonds and the back bonds stem from the benzene π system and there is no symmetry which could prevent these states from interacting with the substrate. The antisymmetric linear combination π_- (which corresponds to $1b_{3g}^{\pi}$ in cyclohexadiene) has a node in the dimer plane, which reduces its back-bond character, but there is significant interaction with the second-layer dimer states.

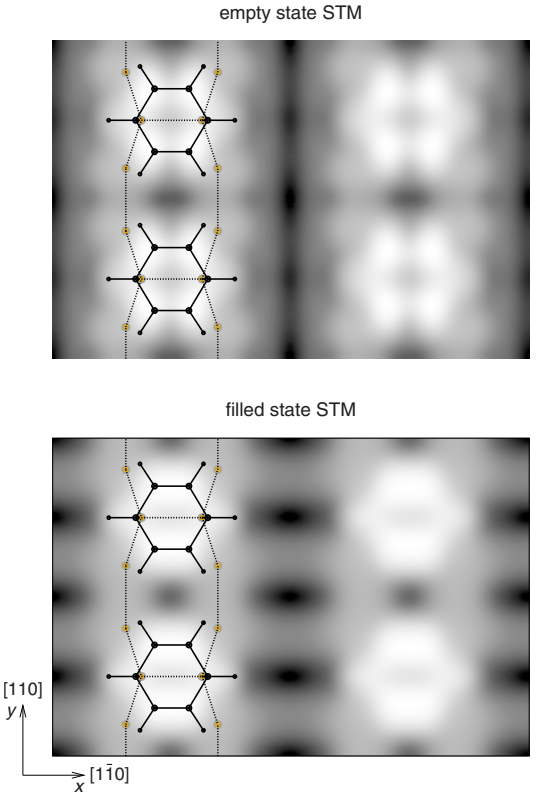

FIG. 6. (Color online) Simulated constant-current STM images of the benzene π^* and π orbitals. In the left half of the figures, the atomic positions of the benzene molecule and the first two Si layers are shown.

The symmetric linear combination π_+ $(2b_{1u}^{\pi})$, in contrast, contributes significantly to the C—Si σ bonds. The symmetric and antisymmetric linear combinations of the antibonding $\pi_{\pm}^*$ orbitals, which interact far less with the substrate, occur between 3 and 3.5 eV.

Figure 5 clearly shows that the empty and occupied dangling bonds of the clean SiC(001)-(3×2) surface[41] become saturated and are thus quenched by adsorption of benzene. The band gap of 0.72 eV of the clean surface opens up to 1.02 eV for the adsorption system. The occupied states S_1 and S_2 localized at the Si dimers on the third layer remain essentially undisturbed upon benzene adsorption, while the antibonding second-layer states[23] rehybridize to a symmetric (B_+) and an antisymmetric (B_-) linear combination due to the mirror symmetry $x\leftrightarrow-x$ of the adsorbate system. This mirror symmetry is missing at the clean surface since the top-layer dimers are asymmetric in that case. The change in the substrate-related bands is very similar to the case of acetylene adsorption in *on top* positions on the same substrate.[23]

To encourage and support experimental scanning tunneling microscopy (STM) studies of benzene on the SiC(001)-(3×2) surface, we have calculated filled- and empty-state STM images in the constant-current mode within the Tersoff-Hamann approximation.[47] Occupied states down to −3 eV and empty states up to 4 eV with respect to the projected valence-band edge have been included. The most prominent features of the empty-state image in the upper

panel of Fig. 6 originate from the antibonding π^* orbitals at the C=C double bonds, which appear as two bright lobes with pronounced intensity minima in their center. The latter are due to the nodal plane of the wave functions in the middle of the C=C double bonds which are not directly involved in bonding of the molecule to the substrate. In the filled-state image, shown in the lower panel of Fig. 6, the bonding π orbitals lead to bright spots at the C=C double bonds without an intensity minimum in the middle since the occupied states do not have a nodal plane. Thus benzene molecules give rise to clearly discernible fingerprints in empty- and filled-state STM images.

IV. SUMMARY

We have investigated benzene adsorption on the SiC(001)-(3×2) surface by DFT-GGA calculations. According to our results, benzene adsorbs on the SiC(001)-(3×2) surface in the standard-butterfly configuration. The asymmetric Si dimers on the top layer of the clean surface become symmetric thereby. For chemisorption, the benzene molecule has to surmount only a small barrier of 0.1 eV. We have discussed the adsorption reaction as an electrophilic addition. For none of the other favorable structural models discussed previously for benzene adsorption on Si(001)-(2×1), a viable reaction pathway is found on SiC(001)-(3×2). Thus it should be possible to achieve a well-ordered monolayer of benzene in SB sites on the SiC(001)-(3×2) surface by self-organization. The surface-band structure of C_6H_6:SiC(001)-(3×2) features 12 occupied σ bands with a dispersion of 0.7 eV at most. The molecular σ states giving rise to these bands are influenced only weakly by adsorption of the molecule. On the contrary, the π states of the molecule are more strongly affected by adsorption since they give rise to the bonding between the molecule and the surface by establishing new C—Si bonds. In the energy region close below the top of the projected valence bands, the remaining π states hybridize with the C—Si back bonds and the second-layer Si dimer states, respectively. While the dangling-bond states of the clean SiC(001)-(3×2) surface are fully quenched by benzene adsorption, the surface states of the clean surface on the second and third layers remain in the projected gap after benzene adsorption. Our simulated STM images suggest that benzene molecules adsorbing in the standard-butterfly configuration on the SiC(001)-(3×2) surface should clearly be identifiable in STM experiments.

ACKNOWLEDGMENT

The structure optimization calculations were carried out on the computers of the Morfeus-GRID at the University of Münster (Germany) using CONDOR (see Ref. 48).

*wieferink@uni-muenster.de

[1] J. T. Yates, Jr., Science **279**, 335 (1998).
[2] S. F. Bent, Surf. Sci. **500**, 879 (2002).
[3] Y. Taguchi, M. Fujisawa, T. Takaoka, T. Okada, and M. Nishijima, J. Chem. Phys. **95**, 6870 (1991).
[4] G. P. Lopinski, D. J. Moffatt, and R. A. Wolkow, Chem. Phys. Lett. **282**, 305 (1998).
[5] G. P. Lopinski, T. M. Fortier, D. J. Moffatt, and R. A. Wolkow, J. Vac. Sci. Technol. A **16**, 1037 (1998).
[6] R. A. Wolkow, G. P. Lopinski, and D. J. Moffatt, Surf. Sci. **416**, L1107 (1998).
[7] B. Borovsky, M. Krueger, and E. Ganz, Phys. Rev. B **57**, R4269 (1998).
[8] S. Gokhale, P. Trischberger, D. Menzel, W. Widdra, H. Dröge, H.-P. Steinrück, U. Birkenheuer, U. Gutdeutsch, and N. Rösch, J. Chem. Phys. **108**, 5554 (1998).
[9] M. J. Kong, A. V. Teplyakov, J. G. Lyubovitsky, and S. F. Bent, Surf. Sci. **411**, 286 (1998).
[10] R. A. Wolkow, Annu. Rev. Phys. Chem. **50**, 413 (1999).
[11] P. L. Silvestrelli, F. Ancilotto, and F. Toigo, Phys. Rev. B **62**, 1596 (2000).
[12] M. Staufer, U. Birkenheuer, T. Belling, F. Nörtemann, N. Rösch, W. Widdra, K. L. Kostov, T. Moritz, and D. Menzel, J. Chem. Phys. **112**, 2498 (2000).
[13] W. A. Hofer, A. J. Fisher, G. P. Lopinski, and R. A. Wolkow, Phys. Rev. B **63**, 085314 (2001).
[14] N. Witkowski, F. Hennies, A. Pietzsch, S. Mattsson, A. Föhlisch, W. Wurth, M. Nagasono, and M. N. Piancastelli, Phys. Rev. B **68**, 115408 (2003).
[15] Y. K. Kim, M. H. Lee, and H. W. Yeom, Phys. Rev. B **71**, 115311 (2005).
[16] N. Witkowski, O. Pluchery, and Y. Borensztein, Phys. Rev. B **72**, 075354 (2005).
[17] J.-Y. Lee and J.-H. Cho, Phys. Rev. B **72**, 235317 (2005).
[18] Y. Jung and M. S. Gordon, J. Am. Chem. Soc. **127**, 3131 (2005).
[19] M. Preuss and F. Bechstedt, Phys. Rev. B **73**, 155413 (2006).
[20] K. Johnston and R. M. Nieminen, Phys. Rev. B **76**, 085402 (2007).
[21] B. Naydenov and W. Widdra, J. Chem. Phys. **127**, 154711 (2007).
[22] K. Johnston, J. Kleis, B. I. Lundqvist, and R. M. Nieminen, Phys. Rev. B **77**, 121404(R) (2008).
[23] J. Wieferink, P. Krüger, and J. Pollmann, Phys. Rev. B **75**, 153305 (2007).
[24] J. Wieferink, P. Krüger, and J. Pollmann, Phys. Rev. B **74**, 205311 (2006).
[25] R. L. Hayes and M. E. Tuckerman, J. Phys. Chem. C **112**, 5880 (2008).
[26] P. Hohenberg and W. Kohn, Phys. Rev. **136**, B864 (1964).
[27] W. Kohn and L. J. Sham, Phys. Rev. **140**, A1133 (1965).
[28] J. P. Perdew and Y. Wang, Phys. Rev. B **45**, 13244 (1992).
[29] L. Kleinman and D. M. Bylander, Phys. Rev. Lett. **48**, 1425 (1982).
[30] S. F. Boys and F. Bernardi, Mol. Phys. **19**, 553 (1970).
[31] S. K. Burger and W. Yang, J. Chem. Phys. **124**, 054109 (2006).
[32] W. E, W. Ren, and E. Vanden-Eijnden, Phys. Rev. B **66**, 052301 (2002).
[33] H. Jónsson, G. Mills, and K. W. Jacobson, *Classical and Quan-*

tum Dynamics in Condensed Phase Simulations (World Scientific, Singapore, 1998), Chap. 16, p. 385.
[34] G. Henkelman, B. P. Uberuaga, and H. Jónsson, J. Chem. Phys. **113**, 9901 (2000).
[35] G. Henkelman and H. Jónsson, J. Chem. Phys. **113**, 9978 (2000).
[36] R. Lindh, A. Bernhardsson, G. Karlström, and P.-Å. Malmqvist, Chem. Phys. Lett. **241**, 423 (1995).
[37] To assess the rate of convergence of the QSM, we have applied the method to the test systems described in Ref. 39, i.e., several arrangements of a Pt-heptamer island on a Pt(111) surface. It turns out that the average number of necessary force calls per image until the forces are smaller than 0.01 or 0.001 eV/Å is 48 or 69, respectively. The most efficient of the algorithms compared in Ref. 39, the global Broyden-Fletcher-Goldfarb-Shanno (BFGS) algorithm without line search, is reported to need 49 or 73 iterations for the same accuracy, respectively.
[38] D. Sheppard, R. Terrell, and G. Henkelman, J. Chem. Phys. **128**, 134106 (2008).
[39] N. Marzari and D. Vanderbilt, Phys. Rev. B **56**, 12847 (1997).
[40] A. A. Mostofi, J. R. Yates, Y.-S. Lee, I. Souza, D. Vanderbilt, and N. Marzari, Comput. Phys. Commun. **178**, 685 (2008).
[41] W. Lu, P. Krüger, and J. Pollmann, Phys. Rev. B **60**, 2495 (1999).
[42] M. D'angelo, H. Enriquez, V. Yu. Aristov, P. Soukiassian, G. Renaud, A. Barbier, M. Noblet, S. Chiang, and F. Semond, Phys. Rev. B **68**, 165321 (2003).
[43] A. Tejeda, D. Dunham, F. J. García de Abajo, J. D. Denlinger, E. Rotenberg, E. G. Michel, and P. Soukiassian, Phys. Rev. B **70**, 045317 (2004).
[44] The interaction energy in the considered precursor is slightly positive (0.07 eV). This is probably due to an unphysically strong intermolecular repulsion in the basically flat benzene monolayer (in a real experiment single molecules adsorb one after another experiencing less intermolecular interaction), for one reason, and also related to the fact that the very small interaction energy is near the accuracy level of the counterpoise correction. The real interaction can be expected to be slightly attractive indeed. In either case, the energy barrier can be surmounted by a considerable fraction of the impinging benzene molecules.
[45] D. F. Shriver, P. W. Atkins, and C. H. Langford, *Anorganische Chemie* (Wiley, New York, 1997).
[46] S. K. Burger and W. Yang, J. Chem. Phys. **127**, 164107 (2007).
[47] J. Tersoff and D. R. Hamann, Phys. Rev. B **31**, 805 (1985).
[48] M. J. Litzkow, M. Livny, and M. W. Mutka, *CONDOR—A Hunter for Idle Workstations*, in Proceedings of the Eighth International Conference on Distributed Computing Systems (IEEE, Washington, D.C., 1988), pp. 104-111.